Mechanism Design and Testing of a Self-Deploying Structure Using Flexible Composite Tape Springs

Joseph N. Footdale[*] and Thomas W. Murphey[**]

Abstract

The detailed mechanical design of a novel deployable support structure that positions and tensions a membrane optic for space imagining applications is presented. This is a complex three-dimensional deployment using freely deploying rollable composite tape spring booms that become load bearing structural members at full deployment. The deployment tests successfully demonstrate a new architecture based on rolled and freely deployed composite tape spring members that achieve simultaneous deployment without mechanical synchronization. Proper design of the flexible component mounting interface and constraint systems, which were critical in achieving a functioning unit, are described. These flexible composite components have much potential for advancing the state of the art in deployable structures, but have yet to be widely adopted. This paper demonstrates the feasibility and advantages of implementing flexible composite components, including the design details on how to integrate with required traditional mechanisms.

Introduction

Current efforts in advancing the art of deployable structures include developing deployment architectures that maximize the packaging efficiency while minimizing mass and satisfying dimensional stability constraints. A number of developed and conceptual architectures are making such advancements with the implementation of flexible Fiber Reinforced Polymer (FRP) composite laminate components in place of traditional hinge and latching mechanisms. The Air Force Research Laboratory (AFRL) Space Vehicles Directorate has developed multiple deployable architectures [1-3], including a boom [4] that employed rollable composite tape spring members. These example structures also utilized the stored strain energy of the structure in the packaged configuration to provide the motive force to drive the deployment, eliminating the need for external energy sources (motors or springs for example). The tape spring members are similar in shape and functionality as the Storable Tubular Extendable Member (STEM) boom [5]. The difference lies in the engineered laminate design that allows the tape spring to tightly wrap around a cylindrical drum without requiring containment mechanisms or shroud to prevent radial billowing during deployment. FRP composite laminates are the preferred material because of the increased strain capability, higher modulus, lower mass, and increased dimensional stability over conventionally used metallic materials for flexure applications.

This paper presents the design and testing of a novel, self-deployable support structure that implements rollable composite tape spring members. The structure is a departure from existing architectures due to the synchronous deployment of the structure in three dimensions simultaneously. The synchronous deployment is achieved without any mechanical components to enforce the desired kinematics. This was accomplished through a combination of a tape spring laminate and geometry and constraint mechanism designs. When compared to the relatively large number of mechanisms and support components required in traditional systems to enable the deployment of a three-dimensional structure, the freely-deploying architecture presented offers significant advantages with respect to complexity (and associated cost) and performance.

[*] LoadPath, Albuquerque, NM

[**] High Strain Dynamics, Phoenix, NY

A CubeSat-scale telescope with a membrane primary optic was selected as an example three-dimensional deployment application to demonstrate the flexible composite technology. The primary objective of this effort was to design the tape springs and determine the required mechanisms to develop a kinematic functional unit. There are many features required for an operational CubeSat payload not designed in detail, such as a primary deployment stage that would be required to translate the telescope from the bus interior such that the extendable booms do not impinge the CubeSat walls. These features were a factor in the design of the deployment mechanism and fixtures of the prototype unit, such that there is a feasible transition from the prototype to a flight system. This is the first known documentation of the fabrication and demonstration of this specific class of a three-dimensional deployable structure featuring flexible composite mechanisms. Two papers [6,7] regarding this structure were previously published and presented that primarily focused on the overall structure and membrane design for the deployable membrane telescope. This paper describes in detail the designs of the mechanisms required to enable successful operation of the structure and aims to serve as a design guide for integrating flexible composite components in existing or conceptual deployable structure architectures. The detail mechanical design of the mechanism is first described. An overview of flexible composite research is then presented along with the tape spring laminate and geometry design. Results of the functional deployment tests are discussed next, followed by the lessons learned from this effort.

Mechanism Design

Design Summary
The telescope design in the deployed and stowed configurations is illustrated in Figure 1. The deployable structure subsystem consists of a planar tri-member frame ("top frame") that is extended from the base mechanism by three deployable booms. Three pull points to tension the membrane was selected because this represents the minimum number to uniquely define a plane. Introducing additional pull points creates an over-determined set that will introduce out-of-plane deformations in the membrane if all points are not precisely located on the nominal plane. The positions of the membrane pull points are controlled by high-stiffness bipedal lanyards at each corner location. The membrane corner pull points are attached to the deployable support structure by high-compliance decoupling spring. Membrane tension is then set by the deployed structure dimensions. A decoupling spring with relatively high compliance reduces the tension sensitivity to the structure dimensional stability. The support structure in this effort was designed to deploy and position a 20-cm-diameter optic with an f-number of 2, and stow within 1U (10 cm x 10 cm x 10 cm) CubeSat volume. The associated compaction ratio to achieve this objective is traceable to the requirements of desired larger diameter applications. The assembled system stows into a volume of 9.4 cm x 9.4 cm x 8.3 cm tall with an assembled mass of 133 g. All tape spring members had a semi-circular cross section and radius of 5.56 mm.

Tape Spring Hub Mechanism
The deployed structure shown in Figure 1 is fully determinant when using only pin-type joints at the tape spring ends. This allows elimination of any latching mechanism for each tape spring at full deployment. The hub mechanism is a simple bearing-supported shaft free to rotate. Exploded and assembled renderings of the top frame hub corner assembly are shown in Figure 2. The tape spring hub assembly is identical for the top frame members and the booms mounted to the base plate. The only difference is in the design of the hub assembly mounting fixture. The central hub disk is fabricated from two pieces that clamp the tape spring end. Hub disk and tape spring components are aligned using two dowel pins and the assembly is bonded with adhesive. The hub disk controls the tape spring roll diameter in the stowed state and mates with the hub shafts, which are concentric with the hub disc. Thickness of the hub disk was kept to a minimum to keep the rotary inertia low during deployment. The geometry and laminate of the FRP composite tape spring are designed such that no containment devices are required to maintain a tight roll of the tape spring around the central hub disk while stowed or during the deployment process. Circumferential and side containment shrouds (circumferential shrouds not shown in Figure 2 for clarity) are included to prevent anomalous deployment events. The side shrouds are circular disks that mounted to the hub shafts and rotate with the tape spring roll. This basic shroud design was first implemented in

the SIMPLE boom [4], which demonstrated effective functionality. The design was adapted for this application. Further details on the tape spring design are described in a later section below.
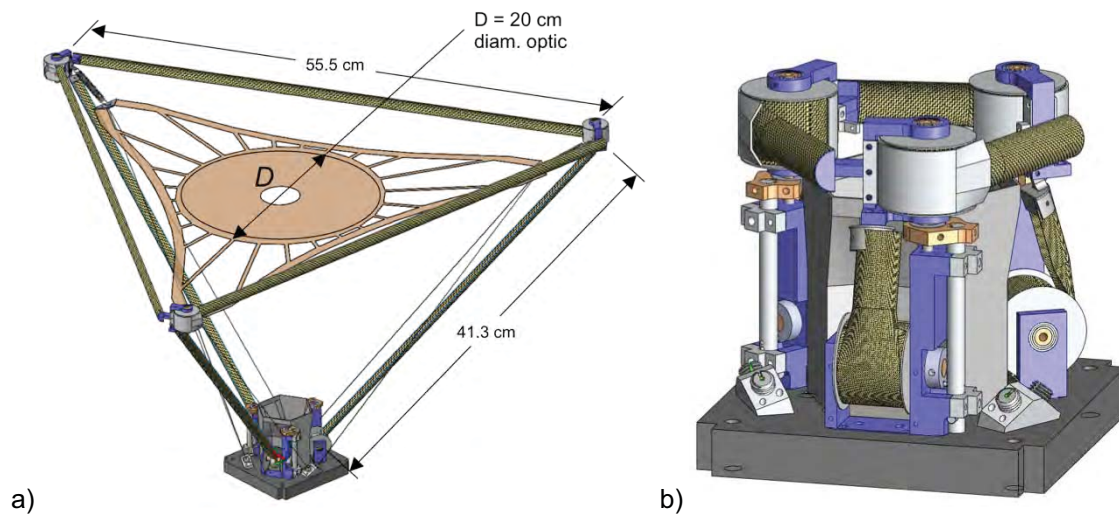
Figure 1. Membrane optic prototype support structure in a) deployed and b) stowed configurations.

Each tape spring is subjected to a compression load at full deployment to react the design tension in the membrane optic. To eliminate the need of a rotation lockout mechanism for the hub assembly at full deployment, the tape spring neutral axis must be coincident with the shaft axis (see Figure 3). This prevents an induced moment at the hub axis from the eccentric loading, which may result in hub rotation if the moment is greater than the tape spring bending stiffness. The same principle determines the required location for the mounting of the adjacent tape spring end, also shown in Figure 3. The intersection of the tape spring neutral axes is coincident with the membrane loading vector, which bisects the angle formed by tape spring neutral axes and is normal to the edge of the membrane end tab.
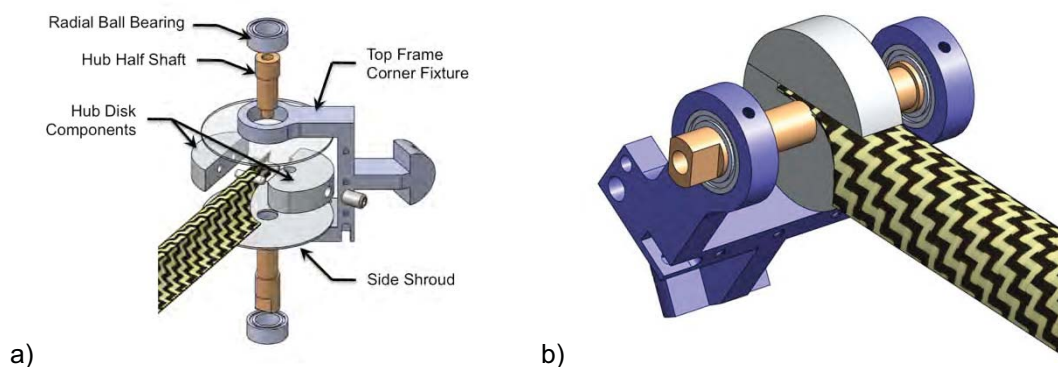

Figure 2. a) Exploded and b) Assembled renderings of top frame corner hub.

The tape spring is located within the central hub to minimize the overall strain in the transition region from the clamped end to the final roll diameter. This mounting position, in addition to constraining the tape spring roll axis to be concentric with the hub shaft axis, results in interference between the tape spring and the hub rotation axis in the fully deployed state. The first option considered, illustrated in Figure 4, eliminates this interference with a U-shaped fixture fastened to the hub disk. This allows the tape spring

to flatten during rolling. The assembly center of gravity was designed to be coincident with the rotation axis as to not induce dynamic imbalance loads during deployments. This design was not selected since the overall width of the hub fixture resulted in the system dimensions to exceed the 1U CubeSat volume requirement.
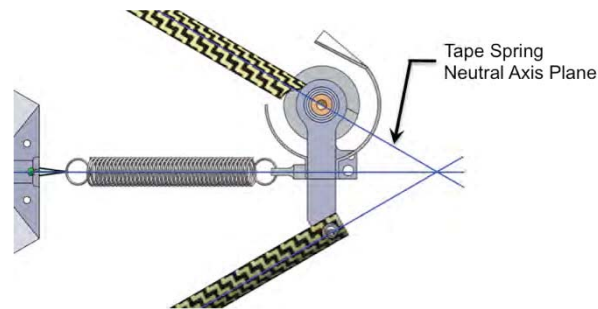
**Figure 3. Top frame tape spring neutral axes locations.**
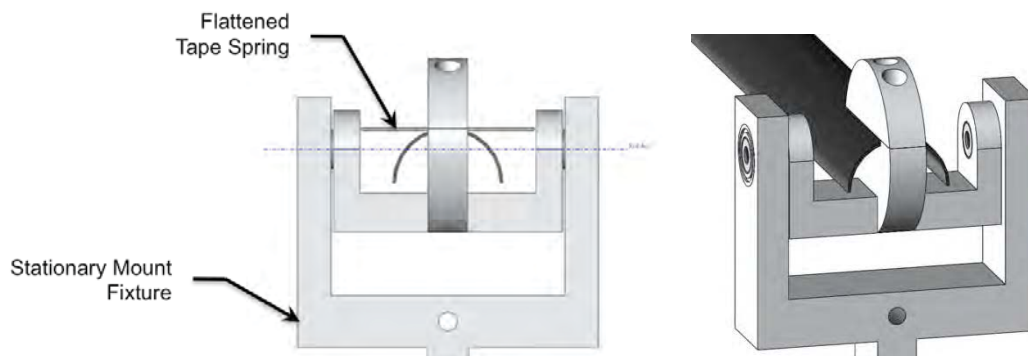
Figure 4. Tape spring hub mechanism design concept requires no clearance trimming

Figure 2b) shows the selected design of trimming the tape spring end to clear the hub shaft. The tape spring clearance cut geometry has a significant effect on the deployment torque and despite only a small reduction in deployed buckling strength [7]. A tight clearance cut, shown in Figure 5a), will maximize these parameters. Fabricated prototypes with this trim profile were observed to have a high failure rate in the radius cut region during rolling of the tape spring. This configuration could be successfully rolled if the tape spring is initially flattened. Sufficient available torque and buckling margins allowed for a more gradual taper cut, shown in Figure 5b), which provided a robust solution capable of repeated stow-deploy cycles without special handling requirements. If the fixture dimensions can be accommodated, it is preferred to have a tape spring with constant cross section, i.e. no clearance trimming.

Constraint/Release Mechanism
In the stowed configuration, the rotation degree of freedom (dof) of each tape spring hub must be constrained until deployment is initiated. The tape spring laminate was designed such that containment fixtures are not required to prevent the tape spring roll from radially billowing out in the stowed state. However, if the free end of the tape spring is held fixed, but the roll rotation dof is unconstrained or opened, the tape spring is in an unstable state and the tape spring roll will begin to rotate. The constraint and release mechanism components to control the deployment for all six tape spring rolls are shown in Figure 6. To prevent binding and have a synchronous deployment, this constraint must be released from all six hubs simultaneously.
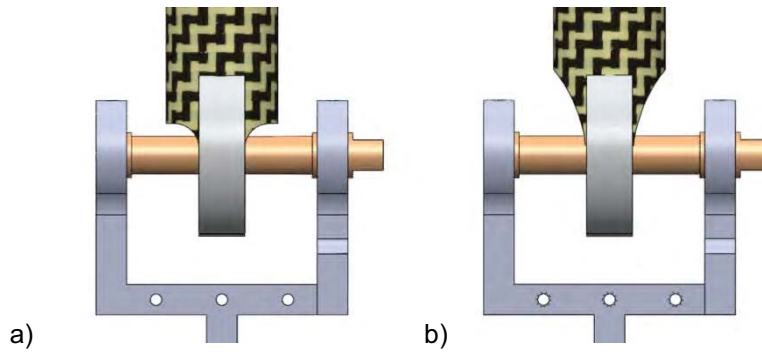
Figure 5. Two example tape spring end clearance cuts.
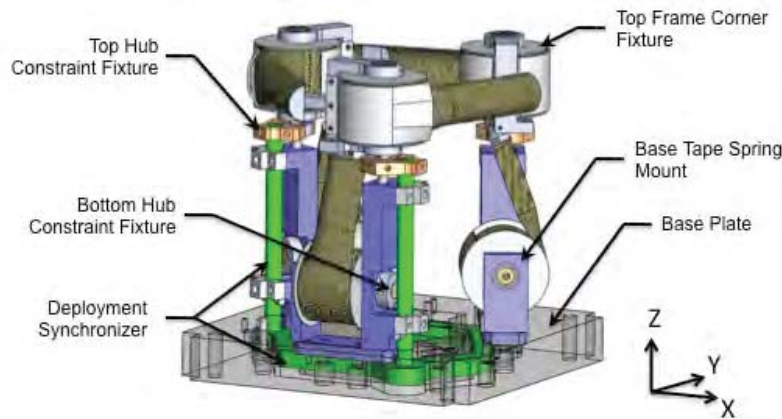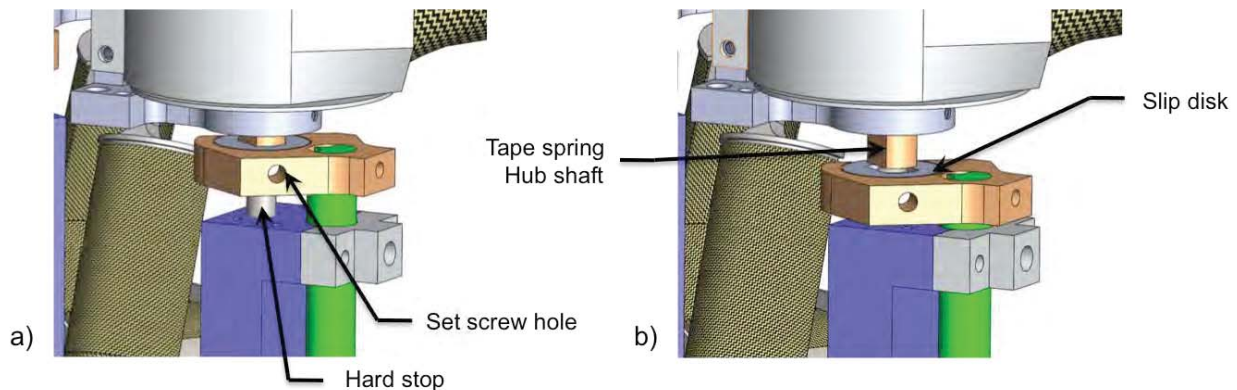

Figure 6. Constraint mechanism components.

The boom tape spring hub fixtures are fastened to the base plate equally spaced 120º apart. Each boom fixture is paired with a top frame tape spring hub assembly, which is positioned above the vertical extension. A cylindrical rod controls the deployment of the pair by vertical (Z-axis) motion. The deployment control rods are mechanically coupled via a rigid ring. For this prototype unit, deployment is initiated by manual actuation of the deployment synchronizer ring. Details for the interface of the deployment control rod and the boom tape spring roll is shown in Figure 7. The tape spring hub half shaft protrudes through the fixture wall. A notched, thin cylindrical disk with a slip fit-sized hole is placed on the shaft. The slip disk also contains a radial tapped hole for a setscrew that mechanically couples/decouples the slip disk from the hub shaft. During tape spring rolling, the setscrew is loosened such that the slip disk can remain stationary. The deployment control rod contains a protruding pin. The rod is actuated vertically such that pin fits within the tape spring notch. Once the tape spring is rolled to the desired length, the setscrew is fastened down. The boom tape spring roll is now locked or constrained. Actuating the control rod vertically down clears the pin from the disk notch, which releases the constraint allowing the tape spring to deploy.
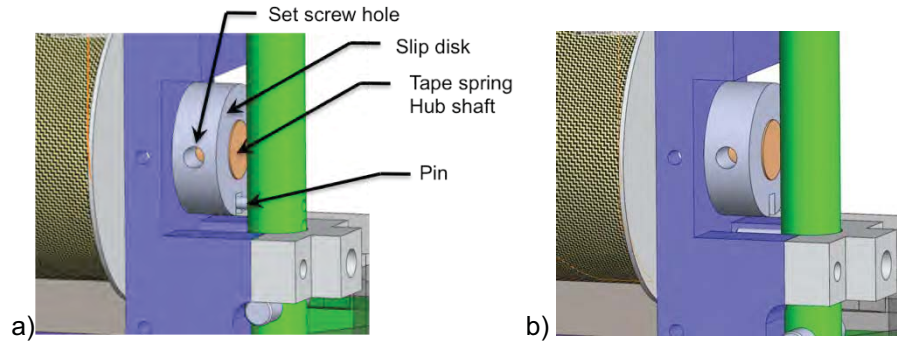
Figure 7. Boom tape spring constraint design in the a) locked and b) released states.

A similar methodology is implemented to control the deployment of the top frame tape spring. The operation and design features of the top frame constraint mechanism are best explained by describing the structure stow procedure. The structure starts in the fully deployed state shown in Figure 1a). The top frame tape springs are simultaneously rolled until the relative distances between the hubs approximate the stowed state shown in Figure 1b). The top frame is temporarily constrained using tape or Velcro applied circumferentially around the assembly. The tape spring booms are then simultaneously rolled until the extending hub shaft (Figure 8b) can be placed into the respective slip disks. The temporary top frame constraint is removed to allow manipulation into the slip disks. The boom tape springs are further rolled such that the top frame hubs are preloaded against the vertical hard stop (Figure 8a). The fixture prevents the top frame from deploying at this stage. Each top frame tape spring is then tightened around the hub disk and held, while setscrews in the constraint fixture (Figure 8a) are fastened to lock the rotation. All tape springs are now fully constrained. Actuating the deployment control rod clears the constraint fixture from the tape spring hub shaft (Figure 8b). The height of the vertical hard stop is set such that the top frame and boom constraints are released simultaneously.

**Figure 8. Top frame hub constraint mechanism design in the a) locked and b) released states.**

Flexible Composite Components

The flexible composites described for deployable structure applications are traditional stiff matrix composites with traditional aerospace-grade resin systems (977-2 and 8552 epoxies, cyanate esters, etc.). The laminate total thickness is kept relatively small such that it can be subjected to large bending strains without failure. The mechanics of flexible FRP composite have been analyzed and tested

extensively. References [8-14] are a small subset of published work on the subject. This section first presents a summary of the fundamental equations used to estimate the rollable tape spring primary characteristics, such as roll radius and deployment torque, that are fabricated from FRP materials. Current and future research in flexible composites that is needed to have a comprehensive understanding of the underlying physics is then discussed. Finally, details of the tape spring design for this effort are reported.

<u>Tape Spring Design Basics</u>
Classical Laminate Theory (CLT) describes the linear-elastic relationship between applied loads and the laminate strains by the **ABD** matrix [15]. The terms of the **ABD** matrix are a function of the lamina material properties and the fiber orientations in the construction. For rollable tape spring applications, the terms in the **D** matrix are of particular interest. AFRL Space Vehicles directorate has developed a general composite laminate construction [10] that exhibits high stiffness, is dimensionally stable, and can be subjected to high strains, which are essential characteristics for this class of tape spring applications. Reference 11 provides further details and high strain flexure test data demonstrating laminate performance. The laminate consists of unidirectional plies sandwiched between bias plain weave plies, as illustrated in Figure 9. The unidirectional lamina stores the primary strain energy upon stowage, which drives the deployment upon release. It is also characterized by high axial stiffness, low susceptibility to creep/relaxation along the fiber direction, and relatively low transverse and shear stiffness. The plain weave lamina provides the required transverse/shear stiffness and contributes to laminate transverse bending stiffness. This significantly increases structural stability of the laminate. Due to the bias orientation, the plain weave lamina is subjected to relatively high shear loads under bending conditions. The viscoelasticity of the matrix significantly factors into the response, resulting in very high susceptibility to creep/relaxation. If solely used in the laminate design, it will fail to deploy due to excessive relaxation.
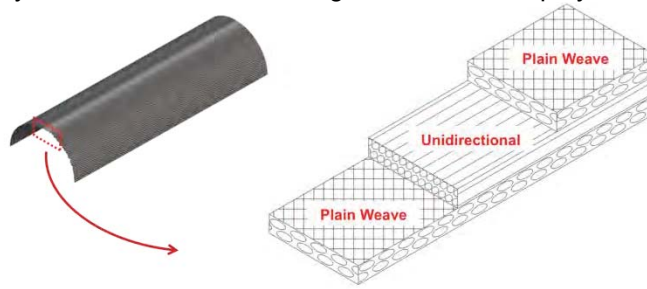
Figure 9. Typical laminate construction for rollable tape springs.

Rollable tape springs are fabricated and strain free in the deployed configuration. The defining geometric characteristics (illustrated in Figure 10) are the cross-section radius, R, subtended angle, β, and overall length, L. Suitable tape spring laminates for this application will have local minimum strain energy state in the rolled configuration in addition to the other local minimum for the deployed state. This property keeps the tape spring from automatically billowing when in the rolled state without constraint. The corresponding inner stowed roll radius, R_s, tends to be approximately equal to the cross-section radius, but can be further estimated by:

$$R_s = R\frac{D_{11}}{D_{12}}$$
(1)

The central hub disk radius, R_H, should be set equal to, or slightly larger than R_s. The tape spring is capable of being wound at a tighter radius without failure, but will billow to the stable radius if not constrained. A strain energy gradient exists between the rolled and the deployed states. To make the tape spring self-deployable, it is constrained in an unstable configuration where free end and rolled sections are in their respective low-energy states. Releasing this constraint allows the tape spring to proceed to the lowest energy state, which is the initial strain-free deployed configuration. The transition is

stable and follows a single kinematic path that manifests as unrolling of the tape-spring. Figure 10 illustrates the transition from the free end that is mechanically held in the deployed state and the tape spring roll section. The unstable transition zone is where the deployment force is generated. Tape spring deployment torque is a weak function of the wrap thickness, which decreases as deployment progresses and is at the minimum right before full deployment where the roll radius is equal to the R_H. The torque value at this state can be roughly approximated by:

$$\tau = \frac{R_H \beta}{2R} \left[D_{22} - \frac{D_{12}^2}{D_{11}} \right] \tag{2}$$

The above equations are used to observe the sensitivity of the stowed radius and deployment torque to the laminate construction and initial geometry to aid in the design process. The predicted performance, determined from either the rigorous calculations, such as described in Ref. 8, or through finite element analyses are naturally only as accurate as the input parameters. For example, the results for thin flexible composites have been shown [11] to be highly sensitive to the lamina thickness terms. Simply using the measured cured thickness can result in a significant over estimation of the available torque. The laminates are designed to be relatively insensitive to creep/relaxation effects; however, torque degradation should be taken into account. One method to approximate the long-term available torque is to assume that the in-plane shear modulus terms (G_{12}) of the plain weave layers is several orders of magnitude less than the initial value found from CLT. Accurate prediction of this degradation is one area of active study in thin flexible composites.
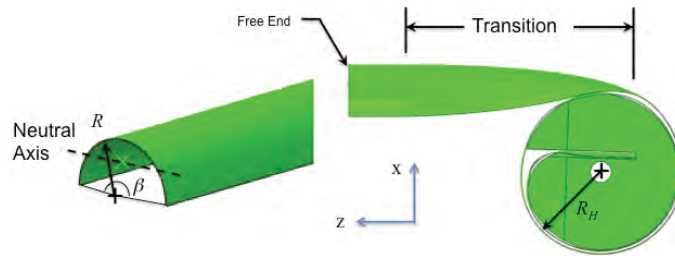
Figure 10. Geometrics definitions of a cylindrical shell.

Current and Future Research in Flexible Composites
The sizeable body of research and development in flexible composite tape springs enables implementation into space deployable architectures with an acceptable level of risk. The components are constructed with space-qualified traditional fibers and material systems to achieve high strains. Also, space-qualified methods are followed to produce consistent, high-quality parts. Engineering methods to predict bending stiffness/deployment torque have been verified [11] to acceptable accuracy. One remaining critical area of current research is to develop the engineering methods to accurately predict flexible composite strength based on stress/strain state for a given laminate. Large deformation bending of composite materials in flexure routinely yield strain levels not attainable by standard ASTM axial tensile test methods. Traditional thick composites ASTM tests fail in compression at lower strains, where the fibers subjection to tensile loads are the failure mode in bending tests. AFRL Space Vehicles directorate has developed a test and analysis methodology to determine stress/strain state at flexural failure [12]. The method constructs a nonlinear constitutive model of the lamina material based on empirical data from a combination of axial and bending tests. With an adequate understanding of lamina nonlinear constitutive behavior, laminate bending response can be predicted and through thickness stresses and strains can be calculated as a function of curvature and at failure. Material failure criteria can then rationally be developed that are pertinent to the large strains achieved in thin flexures.

Experience has shown that traditional CFRP laminates gradually lose strain energy (deployment force) or change dimensions over time while packaged due to stress relaxation. The laminate can be designed to

reduce the degradation, but this results in a high-energy system that results in an unacceptable shock event upon full deployment. Excessive degradation can lead to deployment failure. A simple means to control deployment rate and avoid shock loads has not been developed. Strain energy deployable structures often employ complex mechanisms that control deployment paths and rates using housings, motors and fluid based dampers. These devices can double the system mass, negating any improvements in structural performance and increasing the system and launch costs. A simple material-based solution is currently being investigated, where a CFRP laminate with discrete *elastic* laminas provides deployment force and *viscoelastic* laminas to passively control the deployment rate of the structure. The challenge here is to tailor the net viscoelastic response for deployment rate control. The proposed idea can be thought of as a spring (provided by the low creep elastic lamina) in parallel with a damper (provided by the viscoelastic lamina).

Telescope Structure Tape Spring Design
From previous experience, a composite laminate consisting of an S-2 glass unidirectional fiber sandwich by an Astroquartz plain weave layers at 45º bias has shown good roll stability property with high resistance to creep. The unidirectional lamina was AGY 933-AA-750 S-2 Glass fiber pre-impregnated with Patz Materials & Technolgies PMT-F7 with 10% by weight 3M nanosilicate. The JPS Style 525 Astroquartz II plain weave was also pre-impregnated with the PMT-F7 epoxy. Material properties are listed in Table 1. The effective orthotropic properties for the laminate are presented in Table 2.

Table 1. Tape spring material properties

Property (units)	Astroquartz II/PMT-F7 Plain Weave	S2 Glass/PMT-F7 Unidirectional
E_1 (GPa)	21.7	56.9
E_2 (GPa)	21.7	16.8
G_{12} (GPa)	3.4	6.1
ν_{12}	0.11	0.27
t (mm)	0.1016	0.0762

Table 2. Tape spring laminate properties

| Property (units)	Astroquartz II/PMT-F7 Plain Weave
E_1 (GPa)	21.7
E_2 (GPa)	21.7
G_{12} (GPa)	3.4
ν_{12}	0.11
t (mm)	0.254

The stress in the membrane was a critical design parameter. The membrane design stress level of 68.9 kPa (10 psi) was chosen, which translates to the corner pull-point load of approximately 0.5 N. The load-carrying members in the structure are illustrated in the side view of one corner location in Figure 11. The position of point A in Figure 11 was considered fixed for the initial calculations, which sets the vectors of the membrane force, F_m, and the positioning lanyard force, F_l. The vector of the spring force, F_s, and decoupling spring stiffness, k_s, were varied in a Matlab script to calculate the forces in the top frame and boom tape spring members and their respective lengths. This study gave the position tolerance of point A to maintain F_m within ±0.05 N and the required tape spring cross-section radius to resist buckling with margin. A commercial off-the-shelf extension spring with stiffness of approximately

45.5 N/m with an initial length of 3.2 cm was selected for the prototype unit. A spring force vector that bisects the membrane and lanyard vectors minimized the required minimum tape spring radii. The resulting boom tape spring length was 41.3 cm and is subjected to a compressive load of 0.52 N. The frame tape spring is 55.5 cm in length with a compressive load of 0.27 N.

When sizing the tape spring to resist the compressive loading, the tape spring cross-section was assumed to have a constant radius with a subtended angle of $\beta = \pi$ radians. A half-sine wave shape imperfection with peak amplitude assumed to be 5% of the member length was used to calculate the total load in the member. The minimum tape spring radius was then determined such that the total load in the tape spring was one third of the Euler buckling load. Solving for the top frame and boom cases resulted in the same required minimum tape spring radius of 0.38 cm. However, strain limitations for the layup limit the radius to be greater than 0.48 cm.

The tape spring should have sufficient torque to fully deploy quasi-statically, i.e., not relying on the kinetic energy of the system to assist in the process. A torque margin of 3 was used to calculate the minimum required tape spring cross-section radius to overcome the resistive moment resulting from the axial compressive load in the member. To account for long-term creep effects, the shear modulus in the outer plain weave layers was assumed to be effectively zero. For a constant cross section with $\beta = \pi$ radians, the minimum radius is 0.41 cm. The trimmed tape spring shown in Figure 5b) has an effective subtended angle of $\beta = 0.86$ radian at the root. The resulting minimum radius was 0.54 cm. This was rounded up to a standard mandrel size 0.56 cm (7/16 in) for manufacturing purposes.

A finite element model of the tape spring was created to compare the deployment torque and buckling. Abaqus/Standard was used to perform buckling analyses to compare the buckling loads of the trimmed tape spring geometry to the pristine member. Various trials were performed with initial shape imperfections applied. The trimmed geometry was observed to have a consistent 4% reduction in buckling load capability. A buckling analysis using was then performed by continuously increasing the tension in the compliant member that connects the membrane corner point to the corner of the top triangular frame. The system buckles at an applied load of approximately 48 N, which is two orders of magnitude above the design load of 0.9 N.
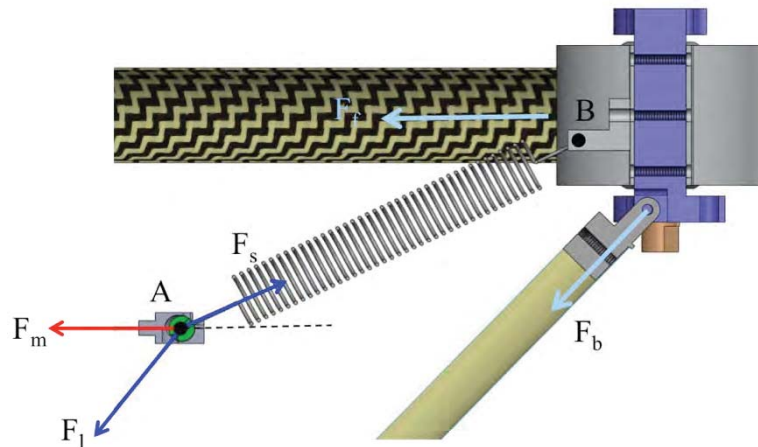
Figure 11. Top frame corner free body diagram.

The central disk radius of 8.5 mm was selected for the hub assembly. The moment generated from the 0.52-N compressive load in the boom tape spring required a deployment torque of at least 4.4 mN-m. The estimated deployment torque from Equation 2 at this radius and taking into account the cross section at

the root due to the clearance trimming was calculated to be 13.3 mN-m. Deployment torque for the untrimmed tape spring is approximately 48.5 mN-m.
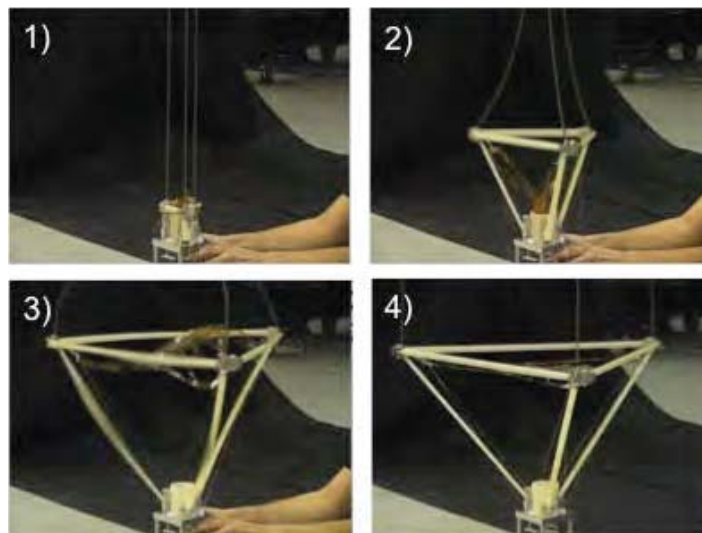
Deployment Testing

The assembled prototype unit is shown in the deployed and stowed configurations in Figure 12. The membrane was cut from 50.8-μm (0.002-inch) thick Kapton using a Gerber ply cutting table. This thickness is approximately 3x that of the anticipated operational material. The positioning lanyards were constructed from braided Spectra cord. The ends were bonded to steel spheres with a hole drilled through the centroid. The membrane was folded in a conical coffee-filter-type fold pattern and guided into the containment shroud located with the tape spring members. Minus the base plate, which was intentionally oversized for testing purposes, the assembled system mass was 113 g.

The initial functional deployment test of the fully assembled structure shown in Figure 12 did not finish in the fully deployed configuration. High-speed video shows the booms would fully deploy, but the shock loading at full deployment caused buckling in the members, at which there was insufficient torque from the boom tape spring members to overcome the compressive load and fully lock out. Manual assistance was given to fully deploy the boom tape springs, which confirmed the system's integrity in the deployed configuration. The boom tape springs were then perturbed to induce buckling and observe the response quasi-statically. The booms did not have sufficient torque to return to the locked state. Original deployment torque calculations did not include parasitic torques from bearing and side shroud friction, or gravitational loading. Preliminary deployment testing without the position control lanyards was successful with no failures observed. Gravity offload support to negate the top frame mechanism mass was included for subsequent testing. The relatively small mass of the corner fixture, coupled with the large vertical deployment distance of 0.26 m, presents a challenge to not overly influence the true dynamics of the deployable structure with a passive offload system. Each top frame fixture was connected to a series of extensional springs with and effective stiffness of 0.28 N/m. The spring ends were connected to a common point approximately 12 m above the test article. Braided Spectra cord was used to connect the springs to the frame fixtures. This height resulted in a negligible parasitic lateral load of approximately 3% of the vertical offload force of 0.19 N. The deviation of vertical offload force from the stowed to the deployed state was roughly 0.07 N (37%). The top frame assembly was disconnected and supported by the offload lines. The height of the upper offload point was adjusted until the top frame was offset at the nominal distance from the base plate. Therefore, the offload system provides additional deployment assistance at the beginning of deployment. The high deployment rate observed in preliminary testing showed sufficient deployment torque was present and the additional force from the offload system was not enabling a deployment that would otherwise fail. After assembly in the deployed state, the booms were manually buckled and returned to the locked state as desired.

Eight deployment tests were performed on the updated test article to demonstrate the feasibility of the novel structure design. Deployments were considered successful if all tape springs fully transitioned to the deployed state and lanyards tensioned as shown in Figure 12. Three attempts resulted in deployment failure, which was due to lanyard snagging on the deployment mechanism. Lanyard control features were not implemented during the first round of testing in order to minimize the effort required to demonstrate deployment feasibility. The membrane containment shroud was redesigned with features to stow the lanyards and provide a more deterministic method to deploy without catching on the mechanism. Four additional deployments were performed with no failures observed. Selected captured images from a successful deployment are presented in Figure 13. The deployment duration was approximately 0.65 second. Deployments were initiated immediately after stowage, such that any torque degradation due to stress relaxation was insignificant. Visual inspection of the tape springs did not reveal any noticeable damage.
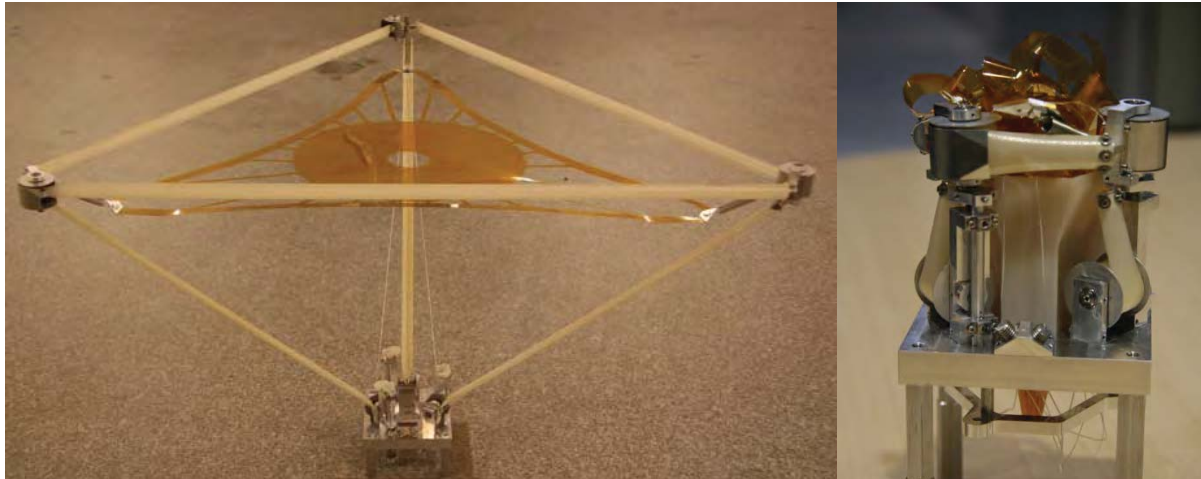
Figure 12. Fabricated structure in the deployed and stowed configurations.

Figure 13. Captured sequence from deployment test

In order to verify the deployable telescope satisfies the structural requirements for an operational system, tests such as deployment repeatability, deployed dimensional stability, and dynamic vibration are needed. Observations from handling and testing of the prototype structure presented a number of departures from a conceived operational unit. The combination of these factors justified reserving the characterization testing for the next structure revision that incorporates the identified design features.

Conclusions

The structure presented in this work incorporated flexible composite tape springs in a novel manner to produce a relatively simple and mass efficient solution for a three-dimensional, self-deployable structure. Through the development process a number of mechanism design requirements were discovered to enable the desired functionality. The tape spring-hub interface design was a driving factor in the overall system design and available torque factor of safety. A hub design that accommodated an untrimmed tape spring did not satisfy the structure volume constraints. Calculations supported the trimmed tape spring end would provide sufficient deployment torque with margin. Gravitational and other parasitic loads

originally unaccounted for, required gravity offload support for ground deployment testing. The off-nominal and inertial loading imparted by the passive offload system yields added uncertainty to the observed structure kinematics. Microgravity testing, or at a minimum active gravity offload support, is suggested for this class of freely deployable structure. The tape springs can be designed to deploy with no gravity offloading, but at the expense of an overly designed system that increases the deployment rate and imparted shock.

Rate control has been a critical design factor in deployable structures. As mentioned previously, a viable rate control solution for this scale of deployable structure is not available. Known methods either add excessive mass and complexity or excessively increase deployment failure risk. The relatively low mass of the deploying structure is a small fraction of a notional 3U CubeSat spacecraft. Free deployment testing of the SIMPLE boom (work not yet published) qualitatively had little impact on bus dynamics. The shock loading on the membrane optic in this application is of larger concern.

The test data required per Reference 11 to more accurately predict the deployment torque was not available for the selected laminate. AFRL Space Vehicles directorate is currently constructing a database of commonly used lamina and laminates to provide this data for future efforts. A test to directly measure the operational tape spring torque over the full deployment would also be beneficial to verify the calculations.

Successful deployment tests were observed to be highly sensitive to simultaneous release of the tape spring rotation constraints. Preliminary functional testing during the design development phase revealed deployment failures often resulted when one top frame hub was released before the other two. Because the top frame deployment does not work against gravity, the rapid motion of the top frame corner fixture would cause the boom tape spring to deploy in a lateral, rather than vertical, fashion that resulted in gross lateral shifting of the top frame assembly. The final hub constraint mechanism using the locking/unlocking slip disk allowed all tape spring rolls to be consistently stowed in a more deterministic fashion against the hard stops and tightly wound about the central hub disk. Proper packaging in this manner was found to be critical for synchronous deployment. The resulting hub and constraint mechanism design enabled repeatable functional three-dimensional deployments. The deployment tests successfully demonstrate that flexible composite tape spring members can be utilized to enable simple and efficient deployable structures.

Acknowledgments

References

1. Mejia-Ariza, J. M., Murphey, T. W., and Dumm, H. P., "Deployable Trusses Based on Large Rotation Flexure Hinges," Journal of Spacecraft and Rockets, Vol. 47, 2010, pp. 1053–1062.
2. Murphey, T. W., Jeon, S. K., Biskner, A., and Sanford, G., "Deployable Booms and Antennas Using Bi-stable Tape- springs," 24th Annual AIAA/USU Conference on Small Satellites, 2010.
3. Pollard, E., Murphey, T. W., and Sanford, G. E., "Experimental and Numerical Analysis of a DECSMAR Structure's Deployment and Deployed Performance," 48th AIAA/ASME/ASCE/AHS/ASC Structures, Structural Dynamics, and Materials Conference, 2007.
4. Jeon, S. K. and Murphey, T. W., "Design and analysis of a meter-class CubeSat boom with a motor-less deployment by bi-stable tape springs," 52nd AIAA/ASME/ASCE/AHS/ASC Structures, Structural Dynamics, and Materials Conference, April 2011.
5. Rimrott, F. P. J. and Fritzsche, G., "Fundamentals of STEM Mechanics," IUTAM-IASS Symposium on Deployable Structures, Theory and Applications, Sep 06-09, 1998.
6. Footdale, J. N. and Murphey, T. W., "Structural Design of a CubeSat-Based Diffractive Optic Telescope," 52nd AIAA/ASME/ASCE/AHS/ASC Structures, Structural Dynamics, and Materials Conference, 2011.
7. Footdale, J. N. and Murphey, T. W., "Design and Testing of Self-Deploying Membrane Optic Support Structure Using Rollable Composite Tape Springs," Proceedings of the 54th AIAA Structures, Structural Dynamics, and Materials Conference, Boston, MA, 2013.
8. Seffen, K. A. and Pellegrino S. "Deployment Dynamics of Tape Springs," Proceedings of the Royal Society London Series A, Vol. 455, pp 1003-1048, 1999.
9. Pellegrino, S., "Bi-Stable Structures," *Deployable Structures*, SpringerWien, New York, 2001, pp. 99-111.
10. Pollard, E. L., and Murphey, T. W., "Development of Deployable Elastic Composite Shape Memory Alloy Reinforced (DECSMAR) Structures," 47th AIAA/ASME/ASCE/AHS/ASC Structures, Structural Dynamics, and Materials Conference, Newport, RI: AIAA, 2006.
11. Peterson, M. E. and Murphey, T. W. "Large Deformation Bending of Thin Composite Tape Spring Laminates," 54th AIAA/ASME/ASCE/AHS/ASC Structures, Structural Dynamics, and Materials Conference, Boston, MA, 2013.
12. Murphey, T. W. and Peterson, M. E., "Four Point Bending of Thin Unidirectional Composite Laminas," 54th AIAA/ASME/ASCE/AHS/ASC Structures, Structural Dynamics, and Materials Conference, Boston, MA, 2013.
13. Domber, J. L., Hinkle, J. D., Peterson, L. D., and Warren, P. A., "Dimensional Repeatability of an Elastically Folded Composite Hinge for Deployed Spacecraft Optics," Journal of Spacecraft and Rockets, Vol. 39, No. 5, pp. 646-652, 2002.
14. Kwok, K. and Pellegrino, S., "Folding, Stowage, and Deployment of Viscoelastic Tape Springs," AIAA Journal, Vol. 51, No. 8, 2013, pp. 1908-1918.
15. Hyer, M. W., Stress Analysis of Fiber-Reinforced Composite Materials, WCB/McGraw-Hill, 1998.